MIT Open Access Articles

Ultrasound-triggered local anaesthesia

Ultrasound-triggered local anaesthesia

Alina Y. Rwei[1,2,†], **Juan L. Paris**[3,4,†], **Bruce Wang**[1], **Weiping Wang**[5], **Christopher D. Axon**[1], **María Vallet-Regí**[3,4], **Robert Langer**[6,7], and **Daniel S. Kohane**[1,8,*]

[1]Department of Anesthesiology, Boston Children's Hospital, Boston, MA 02115, USA

[2]Department of Materials Science and Engineering, Massachusetts Institute of Technology, Cambridge, MA 02139, USA

[3]Dpto. Química Inorgánica y Bioinorgánica, Facultad de Farmacia, UCM, Instituto de Investigación Sanitaria Hospital 12 de Octubre i+12, 28040 Madrid, Spain

[4]Centro de Investigación Biomédica en Red de Bioingeniería, Biomateriales y Nanomedicina (CIBER-BBN), Avenida Monforte de Lemos, 3-5, Madrid 28029, Spain

[5]Dr. Li Dak-Sum Research Centre, The University of Hong Kong - Karolinska Institutet Collaboration in Regenerative Medicine, The University of Hong Kong, Hong Kong, China

[6]David H. Koch Institutes for Integrative Cancer Research, Massachusetts Institute of Technology, Cambridge, MA 02139, US

[7]Department of Chemical Engineering, Massachusetts Institute of Technology, Cambridge, MA 02139, USA

[8]Laboratory for Biomaterials and Drug Delivery, Harvard Medical School, Boston, MA 02115, USA

Abstract

On-demand relief of local pain would allow patients to control the timing, intensity and duration of nerve block in a safe and non-invasive manner. Ultrasound would be a suitable trigger for such a system, as it is in common clinical use and can penetrate deeply into the body. Here, we demonstrate that ultrasound-triggered delivery of an anaesthetic from liposomes allows the timing, intensity and duration of nerve block to be controlled by ultrasound parameters. On insonation, the encapsulated sonosensitizer protoporphyrin IX produces reactive oxygen species that react with the liposomal membrane, leading to the release of the potent local anaesthetic tetrodotoxin. We also show repeatable ultrasound-triggered nerve blocks *in vivo*, with nerve-block duration depending on the extent and intensity of insonation. We did not detect any systemic toxicity, and

*To whom correspondence may be addressed. daniel.kohane@childrens.harvard.edu (D.S. Kohane).
†Authors contributed equally

tissue reaction was benign in all groups. On-demand, personalized local anaesthesia could be beneficial for the managing of relatively localized pain states, and potentially minimize opioid use.

Introduction

Current treatments of perioperative and other forms of relative acute pain are limited, relying heavily on opioids and local anesthetics. Opioids are a mainstay of pain treatments, but are systemic therapies associated with clouding of the sensorium and the potential for tolerance, addiction, diversion, and overdose. Local anesthetics are effective in perioperative and other forms of acute pain, and can be applied throughout a tissue (infiltration local anesthesia), or around a specific nerve or group of nerves (regional anesthesia); in the latter case, they can be effective even when applied at a distance from the injured area or surgical site. However, free local anesthetic solutions tend to be relatively brief in duration. Formulations have been developed that provide approximately one week of nerve block following a single administration[1, 2]. However, drug release from such systems cannot be adjusted in response to changes in the patient's needs. Safe and on-demand local pain relief that allows patients to control the timing, intensity and duration of analgesia according to their changing needs and conditions would have a marked impact on the management of acute pain, and could reduce or obviate the use of opioids.

Remotely-triggered drug delivery systems have been developed that can address the need to modulate pharmacological effects in real time. We have developed injectable on-demand local anesthetic systems[3, 4] that can be triggered by near-infrared light. The difficulty with light as a trigger is that its penetration of tissue may be limited[5]; that limitation may be overcome by increasing the irradiance, but at the risk of causing burns[6, 7].

Ultrasound is non-invasive, can penetrate deep into tissues and it can be applied in a focused manner such that the energy applied in surrounding, non-targeted tissues can be minimized[8, 9]. Ultrasound is already common in clinical practice, for both diagnostic and therapeutic purposes. Nerve block injections are widely guided by ultrasound in the clinic, with an associated reduction in injection-related complications[10] and an increase in success rate[11]. An on-demand nerve block system that could use readily available ultrasound clinical devices might ease clinical translation of on-demand drug delivery systems in pain management.

Many of the current ultrasound-triggerable drug delivery systems, such as micelles[12], liposomes[13], composites[14] and hybrid[15] materials, are responsive to the thermal and mechanical effects of ultrasound waves. Ultrasound can also induce sonochemistry, the use of ultrasound to carry out chemical reactions[16]. Sonodynamic therapy (SDT) has been proposed as an analogous strategy to photodynamic therapy (PDT), in which a sonosensitizer is activated by acoustic energy to generate reactive oxygen species (ROS)[8]. However, the generation of ROS by this effect remains largely unexplored for triggering the release of drugs[17].

Here we developed a liposome-based system to provide ultrasound-triggered repeatable on-demand local anesthesia (Scheme S1). Ultrasound energy encountering the liposomes will

cause a sonosensitizer to release ROS, peroxidating unsaturated lipids in the bilayers, leading to release of local anesthetics which would induce nerve block. As the sonosensitizer[18], we selected protoporphyrin IX (PPIX), a naturally- occurring intermediate of heme biosynthesis[19] and the active component of the FDA-approved pro-drug 5-aminolevulinic acid (ALA)[20]. The hydrophilic site 1 sodium channel blocker, tetrodotoxin (TTX), was chosen as the encapsulated local anesthetic due to its ultra-high potency and minimal myo-[21] and neuro[22]-toxicity. Clinical trials of systemic TTX for cancer pain demonstrated the potential safety of this drug[23, 24].

Results

Liposome preparation and *in vitro* evaluation

PPIX was encapsulated in liposomes consisting of unsaturated lipid (1,2-dilinoleoyl-sn-glycero-3-phosphocholine; DLPC), saturated lipid (1,2-distearoyl-sn-glycero-3-phosphocholine; DSPC), 1,2-distearoyl-sn-glycero-3-phosphatidylglycerol (DSPG), and cholesterol. The mean size was 3.1 ± 0.9 μm (Figure S1). Ultrasound application did not induce statistically significant changes in liposome size (p=0.95, N=4), (Figure S1).

ROS production under insonation was measured by a fluorescent indicator, Carboxy-H2DCFDA. Carboxy-H2DCFDA was added in the liposome solution and the production of ROS upon insonation was measured (Figure 1a); maximal ROS production occurred at a PPIX loading of 0.3% [mg PPIX/mg (PPIX+lipid) $\times$ 100 %]. This ROS production was associated with lipid peroxidation; the extent of peroxidation (see Methods) increased with increasing duration of insonation (Figure 1b). The effect of PPIX loading on ultrasound triggerability of drug release was evaluated in liposomes encapsulating the fluorescent dye sulforhodamine B (Lipo-PPIX-SRho; Figure 1) as reported[4, 25]. Sulforhodamine B (SRho) was loaded into liposomes by hydrating the liposomal lipid cake with a highly concentrated SRho aqueous solution, due to the hydrophilicity of SRho. The dye was encapsulated at a concentration where self-quenching resulted in low fluorescence; once SRho was released, its fluorescence increased, which was measured to determine SRho release. The greatest dye release under ultrasound application ($3W/cm^2$, continuous application, 1 MHz, 10 min) occurred at 0.3 % loading (Figure 1c). In liposomes made with DSPC which is a saturated lipid, instead of the unsaturated and peroxidizable DLPC, dye release from insonation was greatly reduced (Figure 1c, DPLC negative group). Consequently, 0.3 % PPIX was used in all subsequent experiments.

The release of dye from Lipo-PPIX-SRho was dependent on the frequency, duration, intensity and duty cycle of insonation (Figure 1d–f). Based on these results, an ultrasound frequency of 1 MHz, intensity of 3 W/cm^2, and 100% duty cycle were used for subsequent experiments in this study unless otherwise stated. Two durations of insonation were used: 10 min to examine the effect of a single pulse on cargo release, and 5 min when assessing the effects of repeated pulses. (The shorter duration resulted in less release and therefore allowed more triggered events.) Dye release could be repeatedly triggered from liposomes by repeated insonation ($3W/cm^2$, 1 MHz, 5 min; Figure 2a), with up to 4 triggerable events releasing $4.3 \pm 0.8\%$, $4.5 \pm 0.9\%$, $8.2 \pm 2\%$, and $6.0 \pm 0.9\%$ respectively.

To demonstrate that generation of ROS was the likely mechanism of triggered release, we irradiated Lipo-PPIX-SRho (PPIX 0.9 μg/mL, see Methods for details) with 400 nm light, which can cause PPIX to generate reactive oxygen species[26]. Lipo-PPIX-SRho irradiated at 5 mW/cm^2 for 10 min released 9.3% ± 1.8% of their dye payload (Figure S2). Lipo-SRho irradiated under the same conditions released very little dye (Figure S2).

The mechanical properties of blank liposomes (Lipo) and liposomes loaded with PPIX (Lipo-PPIX) were measured using atomic force microscopy (AFM). Liposomes were immobilized on a 3-triethoxysilylpropylamine-functionalized Si wafer and their elastic moduli were measured (see Methods for details). The mean elastic modulus of Lipo was 20.3 ± 6.2 kPa, and that of Lipo-PPIX was 217.3 ± 71.1 kPa (P value comparing the two = 0.00079). These results demonstrate that the addition of PPIX to the liposomal formulation increased the elastic modulus of the liposomal bilayers, i.e. made them less susceptible to mechanical effects of insonation. These results suggest that the release of TTX from Lipo-PPIX is more likely to have been attributable to ultrasound-induced sonochemistry than to the mechanical effects of ultrasound.

The dye-filled liposomes were injected subcutaneously to screen whether the ultrasound-triggered response would function *in vivo*. Subcutaneous application (e.g. for infiltration anesthesia) is only one of many sites at which this system could be used to provide local anesthesia. Ultrasound-triggered release of dye from subcutaneously injected Lipo-PPIX-SRho was demonstrated *in vivo* with an animal fluorescence imaging system (Figure 2b). Upon insonation (3W/cm^2, 1 MHz, 10 min), the fluorescence in the injection area increased by 56 ± 9% (N=4; P < 0.001).

Ultrasound-triggered TTX release *in vitro*

TTX was encapsulated in PPIX-loaded liposomes (Lipo-PPIX-TTX; Figure 3a) with a mean size of 2.8 ± 0.5 μm. The loading efficiencies of TTX and PPIX were 22.2 ±0.2 % and 79.1 ±8.5 % respectively (Table S1), comparable to results from previous studies of TTX loaded liposomes[3].

To confirm that TTX release was also triggerable from PPIX-loaded liposomes, *in vitro* TTX release was assessed by dialyzing 150 μL of Lipo-PPIX-TTX against 14 mL of PBS (Figure 3b–c). 7.1 ±1.0 % of TTX was released within the first 4 h, followed by a slower release of approximately 0.4 %/h (Figure 3b). Ultrasound (3W/cm^2, 1 MHz, 10 min) applied at the 5 h time point induced a release of 5.4 ± 2.6 % of TTX over the next 4 h (Figure 3b). Without ultrasound 1.4 ± 1.0 % was released over the same period. Liposomes loaded with TTX but without PPIX (Lipo-TTX) showed comparable TTX loading to Lipo-PPIX-TTX (Table S1), but TTX release was faster in the absence of PPIX: initial release was 19.6 ± 5.7 % in the first 4 h, after which release leveled off (Figure 3c). Ultrasound applied to Lipo-TTX at the 5 h time point did not trigger TTX release. Comparing the release profile of Lipo-PPIX-TTX and Lipo-TTX, we find that in the first hour, release from Lipo-TTX (Figure 3c) was more than twice that from Lipo-PPIX-TTX (p = 0.02; Figure 3b); by 2 h the difference was almost three-fold (p < 0.01). These results show that PPIX was necessary for ultrasound-triggered TTX release.

Lipo-PPIX-TTX and Lipo-TTX (TTX liposomes without PPIX) were insonated, and TTX was extracted as described[42] and quantified by ELISA. Insonation, and the resulting production of ROS, did not affect the concentration of TTX in Lipo-PPIX-TTX (Figure S3).

Ultrasound-triggered sciatic nerve blockade *in vivo*

Liposomes were injected at the rat sciatic nerve, and nerve blockade was assessed by neurobehavioral testing with a modified hot-plate test (see *Methods* section). In these experiments, the principal metric of nerve block was the thermal latency (the length of time a rat would leave its hindpaw on a hotplate; 2 s was baseline and 12 s was maximal nerve block). In general, block was considered successful if latency was > 7 s. Duration of nerve block was defined as the time for thermal latency to return to 7 s, the mid-point between baseline and maximal block.

Lipo-PPIX-TTX induced an initial nerve block lasting 8.3 ± 4.7 h (N = 4; Table S2, Figure 4a). Insonation ($3W/cm^2$, 1 MHz, 10 min) after the thermal latency returned below 4 s resulted in a return of nerve block for 0.7 ± 0.2 h. A second application of ultrasound, applied after the thermal latency returned to 4 s again, caused a return of nerve block with a duration of 0.2 ± 0.2 h (Figure 4a). No nerve block was observed after a third ultrasound application. There was no animal mortality or increase in latency in the non-injected extremity (an established metric of systemic toxicity[27]). However, 50% of animals injected with Lipo-TTX (3 of 6) died 3–10 h after injection, and 4 out of 6 rats showed an increase in latency in the non-injected extremity, possibly a reflection of the more rapid TTX release in this group (Fig. 3c). In the 3 animals that survived (Figure 4b), Lipo-TTX induced an initial nerve block of 17.2 ± 11.3 h, but insonation after the thermal latency returned below 4 s did not induce renewed nerve block (Figure 4b, P = 0.001 between nerve block duration of Lipo-PPIX-TTX and Lipo-TTX after insonation) or dye release (Figure S4), demonstrating that PPIX was necessary for insonation-induced nerve block and cargo release.

To assess the possibility that a formulation component other than TTX was causing nerve block, rats were injected at the sciatic nerve with PPIX-loaded liposomes without TTX (Lipo-PPIX, Figure S5). Initial injection did not induce nerve block, nor did insonation 8 h after injection, demonstrating that TTX was necessary for nerve block. Animals directly treated with ultrasound in the absence of formulation administration did not develop nerve block upon insonation (Figure S6).

To further demonstrate that the triggerablity of the Lipo-PPIX-TTX was due to ultrasound causing liposome lipid peroxidation, and not due to other effects of ultrasound, we injected rats at the sciatic nerve with TTX-containing liposomes (Lipo-DSPC-TTX) that did not contain PPIX or DLPC (which was replaced by DSPC, which cannot be peroxidated) and therefore could not be triggered in vitro (Figure S7a). Lipo-DSPC-TTX caused an initial nerve block of 6.1 ± 3.6 h, which was comparable to the duration of initial block from Lipo-PPIX-TTX, but insonation did not induce nerve block (Figure S7).

To further enhance the number and duration of ultrasound-triggerable nerve blocks, we co-administered dexmedetomidine-loaded liposomes (Lipo-DMED, see Figure S8 for cryo-TEM image, see *Methods* for synthesis) with Lipo-PPIX-TTX at a 1:2 (Lipo-DMED: Lipo-

PPIX-TTX) mass ratio. Dexmedetomidine, an α_2-adrenergic agonists, prolongs the local anesthetic effects of TTX[28] Lipo-PPIX-TTX + Lipo-DMED caused an initial nerve block of 34.5 ± 5.0 h (Figure 5, Table S2). Repeated insonation (3 W/cm^2, 1 MHz, 10 min) after the return to 4 s latency triggered three separate consecutive nerve blocks with durations of 1.8 ± 1.2 h, 0.9 ± 0.3 h, and 0.5 ± 0.3 h respectively (Figure 5a, Table S2). The fourth ultrasound application induced an increase in hind-paw thermal latency to a mean of 5.3 ± 1.6 s. These results demonstrate that the co-administration of Lipo-DMED and Lipo-PPIX-TTX enhanced the repeatability and duration of nerve block compared to Lipo-PPIX-TTX alone. Administration of free TTX and DMED caused an initial nerve block of 9.27 ± 2.86 h. Insonation after thermal latency returned to 4 s did not cause an increase in thermal latency (Figure S9). This results demonstrate that that the residual free drug was not sufficient to induce nerve block upon insonation. A corollary to that is that ultrasound was not able to change the effect of the drugs so as to achieve nerve block.

The intensity and duration of the ultrasound-triggered nerve blocks could be controlled by varying the intensity and duration of the applied insonation after the initial nerve block from the administration of Lipo-DMED + Lipo-PPIX-TTX wore off (Figure 5b–d, Table S3). Insonation pulses of 2, 5, and 10 -min induced nerve blocks with a mean duration of 0.2 ± 0.2 h, 0.5 ± 0.2 h and 2.3 ± 0.9 h respectively (Figure 5b). Up to five separate consecutive ultrasound-triggerable nerve blocks were achieved by 5-min insonation (Table S3). The mean peak thermal latency was 12 s for 10-min insonations, 9.9 ± 2.5 s for 5-min insonations, and 7.3 ± 1.4 s for 2-min insonations. The survival rate for all rats injected with Lipo-PPIX-TTX (with and without Lipo-DMED; 20 animals in total) was 100%, and no increase in contralateral latency was observed, suggesting no clinically significant systemic distribution of TTX. The duration of the ultrasound-triggered nerve block increased with increasing duration of insonation, with a plateau at 10 min (Figure 5c).

To examine the effect of insonation intensity on ultrasound-triggered nerve block, insonations of different ultrasound intensities (10 min, 1–3W/cm^2) were applied after the initial nerve block wore off (Figure 5d). The intensity and duration of nerve block increased with the intensity of insonation (Figure 5d, Table S4). No effective nerve block occurred below insonation intensities of approximately 1 W/cm^2, above which duration of nerve block increased with ultrasound intensity.

Tissue reaction

In all animals that underwent neurobehavioral testing, the sciatic nerve and surrounding tissues were collected 4 days after the last ultrasound application. Animals administered PPIX-loaded liposomes had reddish-brown (the color of PPIX) liposome deposits surrounding the sciatic nerve (Figure S10), demonstrating accurate liposome injection at the target site. Collected tissues were processed into hematoxylin & eosin-stained slides. All animals injected with liposomes showed mild inflammation at the injection site consistent with previous reports of perineural microparticle injection[29], but minimal inflammation was seen in the adjacent muscle. Foamy macrophages were observed at the injection site, showing particle uptake (Figure S11). All slides were scored for inflammation (0–4) and myotoxicity (0–6; see details in *Methods*). All groups had median inflammation scores of 1

(Figure S11, detailed scores in Table S5). The median myotoxicity score was 0 in all groups (Figure S11, Table S5). Insonation itself (in the absence of liposome administration) caused no significant inflammation (P=0.4 compared with normal tissue), myotoxicity (P=0.4 compared with normal tissue), or signs of other tissue injury (Figure S12) 1h after application. These data indicated that the ultrasound conditions used in this work do not induce tissue injury, immediately after the application, nor in the following four days.

Sciatic nerves were stained with toluidine blue and sectioned. No significant neurotoxicity was observed in any animals (Figure S13).

Ultrasound-guided injection and sonography of liposomes

Ultrasound-guidance has become a standard of practice for peripheral nerve blockade[30]. It would be advantageous if ultrasound could be used both for procedural imaging and subsequent triggering. We assessed whether Lipo-PPIX could be visualized by ultrasound (Figure 6). PPIX-loaded liposomes (Lipo-PPIX) were placed within ultrasonic gel *in vitro* and were imaged with high frequency ultrasound (40 MHz, $I_{SPTA} < 0.08$ W/cm^2). The liposome layer was densely echogenic while the same volume of water was not (Figure 6a). Under the same experimental conditions, the echogenicity of Lipo was similar to that of (Figure S14) Lipo-PPIX. To show that Lipo-PPIX could be imaged at clinical imaging frequencies (2–20 MHz), Lipo-PPIX was successfully imaged with a 20 MHz transducer (Figure S16).

In anesthetized animals, the sciatic nerve was identified under sonography at a tissue depth of approximately 7 mm (Figure S15, Figure 6b). A 23G needle was then advanced beside the sciatic nerve, and Lipo-PPIX was injected. A bright liposome deposit was observed on the sonogram after injection (Figure 6b), showing successful injection and imaging of liposomes at the target site.

Discussion

On-demand local anesthesia would allow patients to control the timing, duration and intensity of pain relief at will, ideally with a safe and non-invasive triggering system. Here we demonstrated that ultrasound allowed on-demand local anesthesia and that the intensity and duration of local anesthesia could be controlled by adjusting the intensity and duration of insonation (Figures 4–5). The system described here with TTX and DMED would provide about 36 hours of continuous initial nerve block, a duration very suitable for many perioperative contexts. It would then allow an additional half-day of on-demand nerve blockade, allowing personalized narcotic-free pain management. It is possible that such systems would mitigate the need for opioid prescription. Further developments of this proof-of-principle system could be designed to provide a shorter or longer initial nerve block, or a greater number of triggerable events, depending on the clinical context and anatomical site.

As ultrasound is commonly used in the clinics, and hand-held therapeutic ultrasound devices are commercially available, controlling pain relief by adjusting the duration of ultrasound provides a simple method for on-demand local anesthesia. Ultrasound has been used safely for therapy at tissue depths of 2.3 to 5 cm[31]. The device used in this study was a commercial

ultrasound employed in physiotherapy under conditions approved for clinical use. No tissue injury was seen.

Ultrasound is a versatile energy source since it would allow image-guided injection, identification of the injectate in situ, confirmation of the appropriate site, and triggering of drug release. One could envision the use of a single ultrasound device by the clinician for pain treatments: using a diagnostic ultrasound setup (higher frequency, lower power) during injection, followed by formulation imaging, then using a therapeutic setup (lower frequency, higher power) to trigger further anesthetic events post-injection.

The hypothesis that sonochemistry and the production of ROS played a major role in ultrasound-triggered cargo release is supported by the observation that liposomes loaded with PPIX produced a higher amount of ROS compared with blank liposomes (Figure 1), and that the incorporation of PPIX was necessary for triggered release of cargo (Figure 1, Figure 3, Figure 4). Production of ROS upon insonation in the presence of sonosensitizers could be due to several mechanisms.[32, 33] Ultrasound-induced cavitation can produce light (sonoluminescence)[32], which could then activate the photosensitizer PPIX to produce ROS. Implosion of ultrasound-induced cavitation bubbles can also induce the formation of sonosensitizer-derived free radicals which generate ROS[34]. All these effects are dependent on inertial cavitation upon insonation[33], which could be induced by the ultrasound conditions used here (3W/cm^2, 1 MHz, continuous wave)[35].

Another possible mechanism of the ultrasound-triggered cargo release may have been the mechanical effect of ultrasound. Liposome disruption by mechanical effects of ultrasound is known to be more efficient at frequencies much lower than those used in this study[36–38]. In this study, we found that PPIX-loaded liposomes (Lipo-PPIX) were more mechanically stable (higher elastic modulus) than liposomes without PPIX (Lipo). This is in agreement with previous studies, where the incorporation of photosensitizers reduced the fluidity (raised the elastic modulus) of lipid membranes[39] perhaps by enhancing hydrophobic interactions in the lipid bilayer, thereby stabilizing the liposomes[25]. The higher mechanical stability of PPIX-loaded liposomes would make them more difficult to be activated by ultrasound-induced mechanical effects. These data suggest that sonochemical effects, not mechanical effects, may have been the major mechanism of ultrasound-triggered release of TTX.

The difference in elastic modulus between Lipo and Lipo-PPIX may also explain their release kinetics shown in Figure 3b and 3c. Decreasing in the fluidity of the lipid bilayer would decrease the rate of cargo release[1]. This is consistent with our observation in Figure 3, where Lipo was found to release its cargo more rapidly than Lipo-PPIX due to the higher fluidity of its lipid bilayers.

The ultrasound triggerability of PPIX-loaded liposomes increased with PPIX loading at low PPIX concentrations, then decreased above a loading capacity of 0.3 % (Figure 1). This observation is consistent with previous reports[25], where it was attributed to an increase in liposomal stability due to the hydrophobicity of the PPIX included in the lipid bilayer. It is also possible that above a certain concentration of PPIX, there is a self-quenching effect that

diminishes the efficacy of PPIX in ROS generation (as has been described for aluminum and zinc phthalocyanines[40, 41]). The formulation that produced the highest amount of ROS was the same formulation that had the highest ultrasound-triggered dye release. These results indicate that the decrease in ultrasound triggerability of formulations with PPIX loadings higher than the optimal PPIX loading may be due to the increase in PPIX-induced liposomal bilayer stability and the decrease in ROS generation of the formulation due to the self-quenching effect of sonosensitizers.

TTX and other compounds[42] that block the sodium channel at a site (site 1) different from that for conventional local anesthetics, have generally been used as scientific tools. However, their potent local anesthetic properties have long been recognized[43], particularly if their systemic toxicity can be curtailed with other drugs[27] or sustained release[1]. Recently, site 1 sodium channel blockers, including TTX and neosaxitoxin, have undergone clinical trials – the latter for peripheral nerve blockade[44, 45].

Particles containing local anesthetics – including those described here – generally serve as a depot, with drugs diffusing from the site of injection to adjacent nerves[46]. The present system could be applied in the same general set of applications as most local anesthetics: throughout the body, either injected throughout tissue planes (infiltration anesthesia) or along specific nerves or groups of nerves (regional anesthesia). In the latter applications, the particle depot is remote from the painful site; analgesia is provided by interruption of nerve signal proceeding to the brain.

We hypothesized that ultrasound-induced TTX release was the main mechanism of ultrasound-triggered nerve block. Modulation of peripheral nerve activity by ultrasound ("neuromodulation")[47] was another potential contributing factor. In our experiments, insonation of animals injected with PPIX-loaded liposomes without TTX did not induce an increase in thermal latency (Figure S5), nor did insonation of uninjected animals (Figure S6). These experiments suggest that ultrasound itself did not cause nerve block in the absence of TTX. Ultrasound did not cause nerve block after recovery of analgesia from TTX + DMED solution (Figure S9) although it did after recovery from Lipo-PPIX-TTX + Lipo-DMED – indicating that the return of nerve block after insonation of Lipo-PPIX-TTX + Lipo-DMED was due to the release of TTX from the liposomes. Moreover, if the return of nerve block were due to a direct effect of ultrasound on free TTX or on nerve, one would have expected the return to occur in both cases since the local concentrations of TTX would be equal, nerve block having just worn off. We cannot exclude the possibility that ultrasound could affect nerve block, only that it did not do so here.

The eventual lack of effect after multiple triggering of PPIX-loaded liposomes in vitro could be attributable to a number of factors. The ultrasound-triggered peroxidation is irreversible, limiting the number of triggerable (peroxidation-dependent) events. Another potential contributing factor is the depletion of drug remaining in the liposomal reservoir due to basal release and repeated triggers. In vivo, it is possible that degradation and/or removal of particles could also play a role.

We sought to improve the performance of the system by increasing the effect of each packet of TTX released. We did so by co-delivering dexmedetomidine (DMED), an α_2-adrenergic agonist that prolongs the therapeutic effects of local anesthetics[28, 48, 49]. Since the DMED was contained in separate liposomes than the TTX, the effect of DMED was likely a pharmacological one rather than due to increased TTX release. DMED increased the duration of the initial nerve block, as well as the duration and number of triggered nerve blocks. (Figure 4–5, Table S2). One potential mechanism of such synergy by DMED's inhibition of hyperpolarization-activated cation current[48]. Another contributing factor is local α_2-adrenergic receptor mediated vasoconstriction[49, 50], which inhibits redistribution of the local anesthetic, maintaining a high local concentration at the target tissue.

Many local anesthetic drug delivery systems continue to release drug after the local effect has ended[58, 59]. The resulting period of subclinical anesthetic release can be very useful: co-delivery of drugs that potentiate the effect of the anesthetic can render the subclinical concentration effective[1, 60, 61]. This was seen here in the marked prolongation of initial block due to the addition of DMED to the formulation. All released drug will eventually enter the systemic circulation and be eliminated, renally in the case of TTX[62]. Of note, the second drug can also be beneficial in mitigating local toxicity of TTX, particularly if it is a local vasoconstrictor, as are α_2-adrenergics agonists[63] such as DMED.

The mild inflammation from liposomes injections is generally considered safe[51 52], and we saw no significant tissue toxicity from the liposomes or insonation (the ultrasound parameters used in this study are used for therapeutic ultrasound[53]). TTX has also been shown to have minimal myo- and neuro-toxicity[21, 22]. PPIX is the active agent of FDA approved drug ALA[54]. The main ROS that are involved in sonosensitization are hydroxyl radicals and singlet oxygen. The former has a half-life of 10^{-9} s and diffusion distance of 0.06 nm[55, 56], the latter has a half-life of 10^{-6} s and diffusion distance of 268 nm[57]. These distances are small compared to the length scales of tissue, suggesting a low likelihood of toxicity, consistent with the results of this study.

Sustained release local anesthetic systems act by continuously releasing doses high enough to be effective over an extended period. Consequently those that can achieve very long durations of effect commonly contain substantial quantities of drug[1, 60]. The sustained release also prevents systemic toxicity; the fact that the drug payload is contained in a vast number of separate particulate compartments is one safeguard against catastrophic dumping of drug with resulting toxicity. Another important safety consideration in translating such systems into humans lies in the difference in size between humans and rats. The dose required for a given local anesthetic endpoint tracks weakly with animal size[64]. In contrast, local anesthetic toxicity tracks fairly linearly with animal size, in proportion to the increased volume of distribution. Therefore the therapeutic index would be expected to increase in larger animals. This was seen in humans who were able to achieve safe prolonged local anesthesia with neosaxitoxin, a compound that acts by a mechanism similar to that of tetrodotoxin[45, 65, 66]. The doses used in those humans would have been uniformly fatal in rats.

Finally, liposomes may have intrinsic echogenic properties that are dependent on their lipid composition, concentration and vesicle structure. Oligo- and multilamellar liposomes, like the ones used in this study, are more echogenic than unilamellar liposomes[67], providing the ability to image them via ultrasound. Here, 40 MHz was used to provide higher resolution imaging to better target the rat sciatic nerve, which is much smaller than that of humans. This imaging frequency is often used in small animal imaging[68]. In the clinic, ultrasound frequencies of 2 – 20 MHz are used for sonography. Our liposomes can be imaged at those frequencies (Figure S16).

We have developed an ultrasound-triggerable, on-demand nerve block system that allows effective control of nerve block duration and intensity simply through the duration and intensity of insonation. Diagnostic ultrasound allowed guided injection and imaging of the formulation, whereas therapeutic ultrasound induced adjustable and repeatable nerve block.

Methods

Liposome preparation

Liposomes were prepared by the thin-film hydration method, as reported[3]. In brief, the lipid formulation [DSPC (Avanti Polar Lipids, Alabaster, AL, USA), DLPC (Avanti Polar Lipids, Alabaster, AL, USA), DSPG (Genzyme, Cambridge, MA, USA), and cholesterol (Sigma, St. Louis, MO, USA) at molar ratio 3:3:2:3], along with the indicated amount of the sonosensitizer PPIX, was dissolved in a solution of chloroform:methanol 9:1. The solvent was evaporated under reduced pressure, and the lipid was redissolved in t-butanol, followed by freeze-drying. The lipid cake was hydrated with PBS, TTX solution (0.375 mg/mL PBS; Abcam, Cambridge, MA, USA), or sulforhodamine B solution (10 mg/mL PBS; Aldrich, St. Louis, MO, USA). After 10 freeze–thaw cycles, the solution was dialyzed against PBS for 48 h in a dialysis tube with a molecular mass cut-off of 1000 kDa. The dialysis media were changed with fresh PBS at least twice a day. Lipo-DMED was made following the same procedure, but with PPIX not included in the formulation and with hydration in 1 mg/mL of DMED in PBS solution.

Liposome characterization

Liposome size was determined with a Beckman Coulter Multisizer 3 (Beckman Coulter, Indianapolis, IN, USA). Liposomal sulforhodamine B content was determined by UV-Vis absorption (λmax = 565 nm) after disrupting the liposomes with octyl β-D-glucopyranoside (OGP) (Sigma-Aldrich, Milwaukee, WI, USA)[3]. Liposomal PPIX content was determined by UV-Vis absorption at 402 nm after disrupting the liposomes in ethanol[69]. Liposomal TTX content was determined by ELISA (Reagen, Moorestown, NJ, USA) after removing the lipid fraction using the Bligh and Dyer method[70].

Reactive oxygen species (ROS) detection

Carboxy-H2DCFDA (Molecular Probes, OR, USA), is a non-fluorescent reagent commercially available for the detection of ROS[71, 72]. Upon exposure to ROS, it undergoes oxidation and forms the the highly fluorescent 2',7'-dichlorofluorescein (DCF), which can be detected upon fluorescence measurements (Scheme S2). Carboxy-H2DCFDA was dissolved

in ethanol and diluted 100 fold in PBS, followed by the addition to liposome suspension to a final concentration of 10 μM. The fluorescence emission at 527 nm (excitation: 493 nm) was monitored after applying ultrasound to 1 mL of the solution at 3 W/cm^2 for 10 min.

Lipid peroxidation

To determine the degree of lipid peroxidation in the system, we followed a reported Fe-based colorimetric method[73]. Briefly, 0.9 mL of a methanolic solution of xylenol orange (100 μM), Fe^{2+} (250 μM), H$_2$SO$_4$ (25 mM) and butylated hydroxytoluene (4 mM) were incubated with 100 μL of sample for 30 min at room temperature. The absorbance at 560 nm was measured.

In vitro release of fluorescent dye

Self-quenching sulforhodamine B was used as a hydrophilic model dye[3]. To measure ultrasound or 400 nm light-triggered release, sulforhodamine B liposomes were diluted 200-fold in PBS. For ultrasound triggered experiments, 1 mL of the suspension was placed in a 20-mL glass vial and sealed with a latex membrane. Ultrasonic gel was then placed between the latex membrane and the ultrasonic source. Ultrasound was applied at the reported power and duration. For light-triggered experiments, the diluted liposome solution was directed exposed under a 400-nm light source for 10 min, 5 mW/cm^2. The fluorescent intensity (excitation/emission: 560/580 nm) was recorded. The release of dye from liposomes upon ultrasound or light exposure was quantified according to the following equation[3]:

$$\text{Cumulative Release } (\%) = \frac{F - F_0}{F_{\text{break}} - F_0} \times 100$$

F = Fluorescence of solution upon ultrasound exposure F$_0$ = Fluorescence of liposome solution prior to ultrasound exposure F$_{\text{break}}$ = Fluorescence of surfactant (octyl β-D-glucopyranoside)-disrupted liposome solution.

Atomic force microscopy

Silicon wafer (Ted Pella, Inc., Redding, CA, USA) was functionalized by 3-Triethoxysilylpropylamine (APTES, Sigma-Aldrich, Milwaukee, WI, USA) using a previously reported method[74]. Liposomes were placed onto the wafer and left settled for 1 h under room temperature. The DNP-10 AFM tip (Bruker Nano Inc., Camarillo, CA, USA) was used. The AFM machine model was MFP-3D Bio (Asylum Research, Goleta, CA, USA). Force curves were measured and analyzed by the computational program Igor Pro (Wavemetrics, Lake Oswego, OR, USA). The Hertzian model was applied to obtain the elastic moduli as previously reported[75].

In vivo imaging with dye-loaded liposomes (Lipo-PPIX-SRho)

Lipo-PPIX-SRho (150μL) was injected subcutaneously and the fluorescence intensity of the released fluorophore was detected and quantified using an *in vivo* imaging system[4] (IVIS spectrum, Caliper Life Sciences, Waltham, MA, USA) before and after ultrasound

application (3W/cm^2, 10 min, 1 MHz), at excitation and emission wavelengths of 535 nm and 580 nm.

In vitro TTX release

TTX release experiments were performed by placing 150 μL of TTX-loaded liposomes into a Slide-A-Lyzer MINI dialysis device (Thermo Scientific, Tewksbury, MA, USA) with a 20,000 MW cut-off. The sample was dialyzed against 14 mL PBS and incubated at 37°C on a platform shaker at 150 rpm (New Brunswick Innova 40, Eppendorf, Hauppauge, NY, USA)[3]. At predetermined intervals, the dialysis solution was exchanged with fresh PBS. To measure the ultrasound-triggerability of the liposomes, ultrasound was applied (3 W/cm^2, 1 MHz) for 10 min at the 5-h time point. TTX concentration was determined by ELISA (Reagen LLC, Moorestown, NJ, USA).

Animal Studies

Animal studies were performed according to protocols approved by the Boston Children's Hospital Animal Care and Use Committee following the guidelines of the International Association for the Study of Pain[76]. Adult male Sprague–Dawley rats (Charles River Laboratories, Wilmington, MA, USA) weighing 300–400 g were housed in groups under a 12-h/12-h light/dark cycle with lights on at 7:00 AM. Animals were randomly assigned to each group. Under brief isoflurane-oxygen anesthesia, the animals were injected with 200 μL of liposomes with or without 100 μL of Lipo-DMED, using a 23G needle. The injection was performed at the sciatic nerve as described[3] with the needle introduced posteromedial to the greater trochanter, then the animals underwent neurobehavioral testing (see following paragraph) at predetermined intervals. Once the initial nerve block wore off, animals were exposed to ultrasound (New Pocket Sonovit, New Age Italia Srl, Lugo, RA, Italy) under brief anesthesia, at the time points and durations described in Results. The process was repeated until there was no further nerve block. Pharmacokinetic studies were performed by injection SRho-loaded liposomes at a dosage of 1.5 mg/kg and constant volume of 200 μL. The blood was processed using a previously reported method[77]. In brief, at predetermined time points, blood was collected from the tail. After centrifugation, the supernatant was collected. Methanol was then added at a 1:1 vol ratio. Samples were settled overnight at 4°C. The supernatant was collected. The concentration of SRho was analyzed by fluorescence (excitation/emission: 560 /580 nm).

Sensory nerve block was examined at different time points by a modified hotplate test (hind-paw thermal latency) as reported[3, 78]. The researcher who performed the neurobehavioral test was blinded to the sample group allocation. The rat's hindpaw was placed on a preheated hot plate at 56 °C. The time until the animal withdrew its paw foot (the thermal latency) was recorded. Animals that did not retract the paw after 12 s were removed manually to prevent thermal injury. 2 s was considered baseline. Durations of sensory block were calculated as the time required for thermal latency to return to 7 s (the middle point between baseline and maximum possible thermal latency). Measurements were repeated three times at each time point, and the median was used for further data analysis.

Histology

Rats were euthanized by carbon dioxide 4 d after the last ultrasound exposure. The sciatic nerve and surrounding tissue were harvested and underwent standard procedures to produce H&E-stained slides, following the same protocol as previously reported[3]. Inflammation and myotoxicity of the samples were scored as reported[79]. All scoring and other histological assessments were performed by an observer (A.Y.R.) blinded as to the nature of the individual samples. The inflammation score was a subjective quantification of severity in which 0 was normal and 4 was severe inflammation. The myotoxicity score was determined based on nuclear internalization and regeneration of myocytes, which are representative characteristics of local anesthetics' myotoxicity. Nuclear internalization was characterized by myocytes having nuclei located away from their usual location at the periphery of the cell. Regeneration was characterized by the presence of shrunken myocytes with basophilic cytoplasm. The scoring scale was as follows: 0 = normal; 1 = perifascicular internalization; 2 = deep internalization (more than five cell layers); 3 = perifascicular regeneration; 4 = deep tissue regeneration (more than five cell layers); 5 = hemifascicular regeneration; 6 = holofascicular regeneration.

Nerve tissue was processed with toluidine blue staining as previously reported[3]. In brief, the sciatic nerve tissues were fixed in Karnovsky's KII Solution (2.5 % glutaraldehyde, 2.0 % paraformaldehyde, 0.025 % calcium chloride in 0.1 M cacodylate buffer, pH 7.4), followed by postfixation with osmium tetroxide. Samples were then stained with uranyl acetate, dehydrated in graded ethanol solutions, and infiltrated with propylene oxide/TAAB 812 Resin (TAAB Laboratories, Aldermaston, Berks, United Kingdom) mixtures. Tissue sections were stained with toluidine blue.

Ultrasound imaging

The Visualsonics Vevo 2100 (VisualSonics Inc., Toronto, ON, Canada) with an MS-550D 40 MHz or an MS-250 20 MHz transducer at B-mode was used for sonography. *In vitro* imaging was achieved by applying 100 μL of liposome or water on top of a layer of ultrasonic gel, and covering it with another layer of gel. The top layer gel was in contact with the transducer.

Sprague–Dawley rats of 300 – 400 g were anesthetized with isoflurane-oxygen and positioned under the ultrasound transducer. Ultrasonic gel was applied between the transducer and the rat. A 23G needle was used to inject 200 μL of Lipo-PPIX. The needle was placed beside the sciatic nerve as shown from the real-time sonogram prior to liposome administration (Fig. S6).

Statistical Analysis

Statistical comparisons were performed using the Student t-test (one-sided) unless stated otherwise. The variance between the groups that were statistically compared was similar. Thermal latencies, inflammation and myotoxicity scores were reported by medians and quartiles due to its ordinal or non-Gaussian character. All other data were described by means and standard deviations.

Supplementary Material

Refer to Web version on PubMed Central for supplementary material.

References

1. Epstein-Barash H, et al. Prolonged duration local anesthesia with minimal toxicity. Proc. Natl. Acad. Sci. USA. 2009; 106:7125–7130. [PubMed: 19365067]

2. McAlvin, JB., Kohane, DS. Focal Controlled Drug Delivery. Domb, AJ., Khan, W., editors. Springer US; 2014. p. 653-677.

3. Rwei AY, et al. Repeatable and adjustable on-demand sciatic nerve block with phototriggerable liposomes. Proc. Natl. Acad. Sci. USA. 2015; 112:15719–15724. [PubMed: 26644576]

4. Zhan C, et al. Phototriggered local anesthesia. Nano Lett. 2016; 16:177–181. [PubMed: 26654461]

5. Stolik S, Delgado JA, Pérez A, Anasagasti L. Measurement of the penetration depths of red and near infrared light in human "ex vivo" tissues. J. Photochem. Photobiol., B. 2000; 57:90–93. [PubMed: 11154088]

6. Rwei AY, Wang W, Kohane DS. Photoresponsive nanoparticles for drug delivery. Nano Today. 2015; 10:451–467. [PubMed: 26644797]

7. Smalley PJ. Laser safety: risks, hazards, and control measures. Laser Ther. 2011; 20:95–106. [PubMed: 24155518]

8. Wood AK, Sehgal CM. A review of low-intensity ultrasound for cancer therapy. Ultrasound Med. Biol. 2015; 41:905–928. [PubMed: 25728459]

9. Sirsi SR, Borden MA. State-of-the-art materials for ultrasound-triggered drug delivery. Adv. Drug Delivery Rev. 2014; 72:3–14.

10. Marhofer P, Chan VWS. Ultrasound-guided regional anesthesia: current concepts and future trends. Anesth. Analg. 2007; 104:1265–1269. [PubMed: 17456684]

11. Abrahams MS, Aziz MF, Fu RF, Horn JL. Ultrasound guidance compared with electrical neurostimulation for peripheral nerve block: a systematic review and meta-analysis of randomized controlled trials. Br. J. Anaesth. 2009; 102:408–417. [PubMed: 19174373]

12. Li F, Xie C, Cheng Z, Xia H. Ultrasound responsive block copolymer micelle of poly (ethylene glycol)–poly (propylene glycol) obtained through click reaction. Ultrason. Sonochem. 2016; 30:9–17. [PubMed: 26703197]

13. Lin C-Y, Javadi M, Belnap DM, Barrow JR, Pitt WG. Ultrasound sensitive eLiposomes containing doxorubicin for drug targeting therapy. Nanomedicine. 2014; 10:67–76. [PubMed: 23845926]

14. Kim HJ, Matsuda H, Zhou H, Honma I. Ultrasound-triggered smart drug release from a poly (dimethylsiloxane)–mesoporous silica composite. Adv. Mater. 2006; 18:3083–3088.

15. Paris JL, Cabañas MV, Manzano M, Vallet-Regí M. Polymer-grafted mesoporous silica nanoparticles as ultrasound-responsive drug carriers. ACS nano. 2015; 9:11023–11033. [PubMed: 26456489]

16. Cintas P, Tagliapietra S, Caporaso M, Tabasso S, Cravotto G. Enabling technologies built on a sonochemical platform: challenges and opportunities. Ultrason. Sonochem. 2015; 25:8–16. [PubMed: 25547851]

17. Shi J, et al. Reactive oxygen species - manipulated drug release from a smart envelope-type mesoporous titanium nanovehicle for tumor sonodynamic-chemotherapy. ACS Appl. Mater. Interfaces. 2015; 7:28554–28565. [PubMed: 26587885]

18. Kuroki M, et al. Sonodynamic therapy of cancer using novel sonosensitizers. Anticancer Res. 2007; 27:3673–3677.

19. Kennedy JC, Pottier RH. Endogenous protoporphyrin IX, a clinically useful photosensitizer for photodynamic therapy. J. Photochem. Photobiol., B. 1992; 14:275–292. [PubMed: 1403373]

20. Jeffes EWB. Levulan (R): the first approved topical photosensitizer for the treatment of actinic keratosis. J. Dermatol. Treat. 2002; 13:S19–S23.

21. Padera RF, Tse JY, Bellas E, Kohane DS. Tetrodotoxin for prolonged local anesthesia with minimal myotoxicity. Muscle Nerve. 2006; 34:747–753. [PubMed: 16897761]

22. Sakura S, Bollen AW, Ciriales R, Drasner K. Local anesthetic neurotoxicity does not result from blockade of voltage-gated sodium channels. Anesth. Analg. 1995; 81:338–346. [PubMed: 7618726]

23. Hagen NA, et al. Tetrodotoxin for Moderate to Severe Cancer-Related Pain: A Multicentre, Randomized, Double-Blind, Placebo-Controlled, Parallel-Design Trial. Pain Research and Management. 2017; 2017:7.

24. Hagen NA, et al. A multicentre open-label safety and efficacy study of tetrodotoxin for cancer pain. Current Oncology. 2011; 18:E109–E116. [PubMed: 21655148]

25. Carter KA, et al. Porphyrin-phospholipid liposomes permeabilized by near-infrared light. Nat. Commun. 2014; 5

26. Ericson MB, Wennberg A-M, Larkö O. Review of photodynamic therapy in actinic keratosis and basal cell carcinoma. Therapeutics and Clinical Risk Management. 2008; 4:1–9. [PubMed: 18728698]

27. Kohane DS, et al. A re-examination of tetrodotoxin for prolonged duration local anesthesia. Anesthesiology. 1998; 89:119–131. [PubMed: 9667302]

28. McAlvin JB, et al. Corneal anesthesia with site 1 sodium channel blockers and dexmedetomidine. Invest. Ophthalmol. Vis. Sci. 2015; 56:3820–3826. [PubMed: 26066750]

29. Kohane DS, et al. Biocompatibility of lipid-protein-sugar particles containing bupivacaine in the epineurium. J. Biomed. Mater. Res. 2002; 59:450–459. [PubMed: 11774302]

30. Marhofer P, Harrop-Griffiths W, Willschke H, Kirchmair L. Fifteen years of ultrasound guidance in regional anaesthesia: Part 2-Recent developments in block techniques. Br. J. Anaesth. 2010; 104:673–683. [PubMed: 20418267]

31. Hayes BT, Merrick MA, Sandrey MA, Cordova ML. Three-MHz ultrasound heats deeper into the tissues than originally theorized. Journal of Athletic Training. 2004; 39:230–234. [PubMed: 15496991]

32. Kuroki M, et al. Sonodynamic therapy of cancer using novel sonosensitizers. Anticancer Research. 2007; 27:3673–3677.

33. Rosenthal I, Sostaric JZ, Riesz P. Sonodynamic therapy—a review of the synergistic effects of drugs and ultrasound. Ultrasonics Sonochemistry. 2004; 11:349–363. [PubMed: 15302020]

34. MiŠÍK V, Riesz P. Free Radical Intermediates in Sonodynamic Therapy. Annals of the New York Academy of Sciences. 2000; 899:335–348. [PubMed: 10863551]

35. Leighton TG, Pickworth MJW, Walton AJ, Dendy PP. Studies of the cavitational effects of clinical ultrasound by sonoluminescence: 1. Correlation of sonoluminescence with the standing wave pattern in an acoustic field produced by a therapeutic unit. Physics in Medicine and Biology. 1988; 33:1239.

36. Pong M, et al. In vitro ultrasound-mediated leakage from phospholipid vesicles. Ultrasonics. 2006; 45:133–145. [PubMed: 16979206]

37. Schroeder A, Kost J, Barenholz Y. Ultrasound, liposomes, and drug delivery: principles for using ultrasound to control the release of drugs from liposomes. Chem Phys Lipids. 2009; 162:1–16. [PubMed: 19703435]

38. Lin H-Y, Thomas JL. Factors Affecting Responsivity of Unilamellar Liposomes to 20 kHz Ultrasound. Langmuir. 2004; 20:6100–6106. [PubMed: 15248690]

39. Voszka I, et al. Interaction of photosensitizers with liposomes containing unsaturated lipid. Chemistry and Physics of Lipids. 2007; 145:63–71. [PubMed: 17118350]

40. Lyubimtsev A, et al. Aggregation behavior and UV-vis spectra of tetra-and octaglycosylated zinc phthalocyanines. J. Porphyrins Phthalocyanines. 2011; 15:39–46.

41. Rokitskaya TI, Block M, Antonenko YN, Kotova EA, Pohl P. Photosensitizer binding to lipid bilayers as a precondition for the photoinactivation of membrane channels. Biophys. J. 2000; 78:2572–2580. [PubMed: 10777753]

42. Kohane DS, et al. The Local Anesthetic Properties and Toxicity of Saxitonin Homologues for Rat Sciatic Nerve Block In Vivo. Reg. Anesth. Pain Med. 2000; 25:52–59. [PubMed: 10660241]

43. Adams HJ, Blair MRJ, Takman BH. The local anesthetic activity of tetrodotoxin alone and in combination with vasoconstrictors and local anesthetics. Anesth. Analg. 1976; 55:568–573. [PubMed: 1085112]

44. Hagen NA, et al. A multicentre open-label safety and efficacy study of tetrodotoxin for cancer pain. Curr. Oncol. 2011; 18:E109–E116. [PubMed: 21655148]

45. Lobo K, et al. A Phase 1, dose-escalation, double-blind, block-randomized, controlled Trial of safety and efficacy of neosaxitoxin alone and in combination with 0.2% bupivacaine, with and without epinephrine, for cutaneous anesthesia. Anesthesiology. 2015; 123:873–885. [PubMed: 26275090]

46. Kohane DS. Microparticles and nanoparticles for drug delivery. Biotechnology and Bioengineering. 2007; 96:203–209. [PubMed: 17191251]

47. Omer, Naor, Steve, Krupa, Shy, S. Ultrasonic neuromodulation. Journal of Neural Engineering. 2016; 13:031003. [PubMed: 27153566]

48. Brummett CM, Hong EK, Janda AM, Amodeo FS, Lydic R. Perineural dexmedetomidine added to ropivacaine for sciatic nerve block in rats prolongs the duration of analgesia by blocking the hyperpolarization-activated cation current. Anesthesiology. 2011; 115:836–843. [PubMed: 21666435]

49. Yoshitomi T, et al. Dexmedetomidine enhances the local anesthetic action of lidocaine via an alpha-2A adrenoceptor. Anesth. Analg. 2008; 107:96–101. [PubMed: 18635472]

50. Yabuki A, et al. Locally injected dexmedetomidine induces vasoconstriction via peripheral alpha-2A adrenoceptor subtype in guinea pigs. Reg. Anesth. Pain Med. 2014; 39:133–136. [PubMed: 24448513]

51. Richard BM, et al. The safety of EXPAREL (bupivacaine liposome injectable suspension) administered by peripheral nerve block in rabbits and dogs. J. Drug Delivery. 2012; 2012:962101.

52. Vanrooijen N, Vannieuwmegen R. Liposomes in immunology - multilamllar phosphatidylcholine liposomes as a simple, biodegradable and harmless adjuvant without any immunogenic activity of its own. Immunol. Commun. 1980; 9:243–256. [PubMed: 7399568]

53. Rosenberg GJ, Cabrera RC. External ultrasonic lipoplasty: an effective method of fat removal and skin shrinkage. Plast. Reconstr. Surg. 2000; 105:785–791. [PubMed: 10697193]

54. Pudroma X, Moan J, Ma L-W, Iani V, Juzeniene A. A comparison of 5-aminolaevulinic acid- and its heptyl ester: dark cytotoxicity and protoporphyrin IX synthesis in human adenocarcinoma WiDr cells and in athymic nude mice healthy skin. Exp. Dermatol. 2009; 18:985–987. [PubMed: 19469901]

55. Roots R, Okada S. Estimation of life times and diffusion distances of radicals involved in X-ray-induced DNA strand breaks or killing of mammalian-cells. Radiat. Res. 1975; 64:306–320. [PubMed: 1197641]

56. Pryor WA. Oxyradicals and related species - their formation, lifetimes, and reactions. Annu. Rev. Physiol. 1986; 48:657–667. [PubMed: 3010829]

57. Skovsen E, Snyder JW, Lambert JDC, Ogilby PR. Lifetime and diffusion of singlet oxygen in a cell. J. Phys. Chem. B. 2005; 109:8570–8573. [PubMed: 16852012]

58. Curley J, et al. Prolonged regional nerve blockade. Injectable biodegradable bupivacaine/polyester microspheres. Anesthesiology. 1996; 84:1401–1410. [PubMed: 8669682]

59. Kohane DS, Lipp M, Kinney RC, Lotan N, Langer R. Sciatic Nerve Blockade with Lipid-Protein-Sugar Particles Containing Bupivacaine. Pharmaceutical Research. 2000; 17:1243–1249. [PubMed: 11145230]

60. Castillo J, et al. Glucocorticoids prolong rat sciatic nerve blockade in vivo from bupivacaine microspheres. Anesthesiology. 1996; 85:1157–1166. [PubMed: 8916834]

61. Kohane DS, et al. Prolonged duration local anesthesia from tetrodotoxin-enhanced local anesthetic microspheres. Pain. 2003; 104:415–421. [PubMed: 12855352]

62. Lago J, Rodriguez LP, Blanco L, Vieites JM, Cabado AG. Tetrodotoxin, an Extremely Potent Marine Neurotoxin: Distribution, Toxicity, Origin and Therapeutical Uses. Marine Drugs. 2015; 13:6384–6406. [PubMed: 26492253]

63. Kohane DS, Lu NT, Cairns BE, Berde CB. Effects of adrenergic agonists and antagonists on tetrodotoxin-induced nerve block. Regional Anesthesia and Pain Medicine. 2001; 26:239–245. [PubMed: 11359223]

64. Kohane DS, et al. Sciatic nerve blockade in infant, adolescent, and adult rats: a comparison of ropivacaine with bupivacaine. Anesthesiology. 1998; 89:1199–1208. [PubMed: 9822009]

65. Rodriguez-Navarro AJ, et al. Potentiation of Local Anesthetic Activity of Neosaxitoxin with Bupivacaine or Epinephrine: Development of a Long-Acting Pain Blocker. Neurotoxicity Research. 2009; 16:408. [PubMed: 19636660]

66. Rodríguez-Navarro AJ, et al. Comparison of neosaxitoxin versus bupivacaine via port infiltration for postoperative analgesia following laparoscopic cholecystectomy: A randomized, double-blind trial. Reg. Anesth. Pain Med. 2011; 36

67. Alkan-Onyuksel H, et al. Development of Inherently Echogenic Liposomes as an Ultrasonic Contrast Agent†. Journal of Pharmaceutical Sciences. 1996; 85:486–490. [PubMed: 8742939]

68. Shung KK. High Frequency Ultrasonic Imaging. Journal of medical ultrasound. 2009; 17:25–30. [PubMed: 20445825]

69. Jaafar-Maalej C, Diab R, Andrieu V, Elaissari A, Fessi H. Ethanol injection method for hydrophilic and lipophilic drug-loaded liposome preparation. J. Liposome Res. 2010; 20:228–243. [PubMed: 19899957]

70. Bligh EG, Dyer WJ. A rapid method of total lipid extraction and purification. Can. J. Biochem. Physiol. 1959; 37:911–917. [PubMed: 13671378]

71. Da Costa MMJ, et al. A new zebrafish model produced by TILLING of SOD1-related amyotrophic lateral sclerosis replicates key features of the disease and represents a tool for in vivo therapeutic screening. Disease Models & Mechanisms. 2014; 7:73. [PubMed: 24092880]

72. Wu D, Yotnda P. Production and Detection of Reactive Oxygen Species (ROS) in Cancers. J. Vis. Exp. 2011:e3357.

73. Jiang Z-Y, Woollard AC, Wolff SP. Lipid hydroperoxide measurement by oxidation of Fe2+ in the presence of xylenol orange. Comparison with the TBA assay and an iodometric method. Lipids. 1991; 26:853–856. [PubMed: 1795606]

74. Rouhi N, Jain D, Zand K, Burke PJ. Nanotech. 2010; 1:180–182.

75. Liang X, Mao G, Ng KYS. Mechanical properties and stability measurement of cholesterol-containing liposome on mica by atomic force microscopy. Journal of Colloid and Interface Science. 2004; 278:53–62. [PubMed: 15313637]

76. Zimmermann M. Ethical guidelines for investigations of experimental pain in conscious animals. Pain. 1983; 16:109–110. [PubMed: 6877845]

77. Rwei AY, Zhan C, Wang B, Kohane DS. Multiply repeatable and adjustable on-demand phototriggered local anesthesia. Journal of Controlled Release. 2017; 251:68–74. [PubMed: 28153763]

78. Thalhammer J, Vladimirova M, Bershadsky B, Strichartz G. Neurologic evaluation of the rat during sciatic nerve block with lidocaine. Anesthesiology. 1995; 82:1013–1025. [PubMed: 7717536]

79. McAlvin JB, et al. Multivesicular liposomal bupivacaine at the sciatic nerve. Biomaterials. 2014; 35:4557–4564. [PubMed: 24612918]
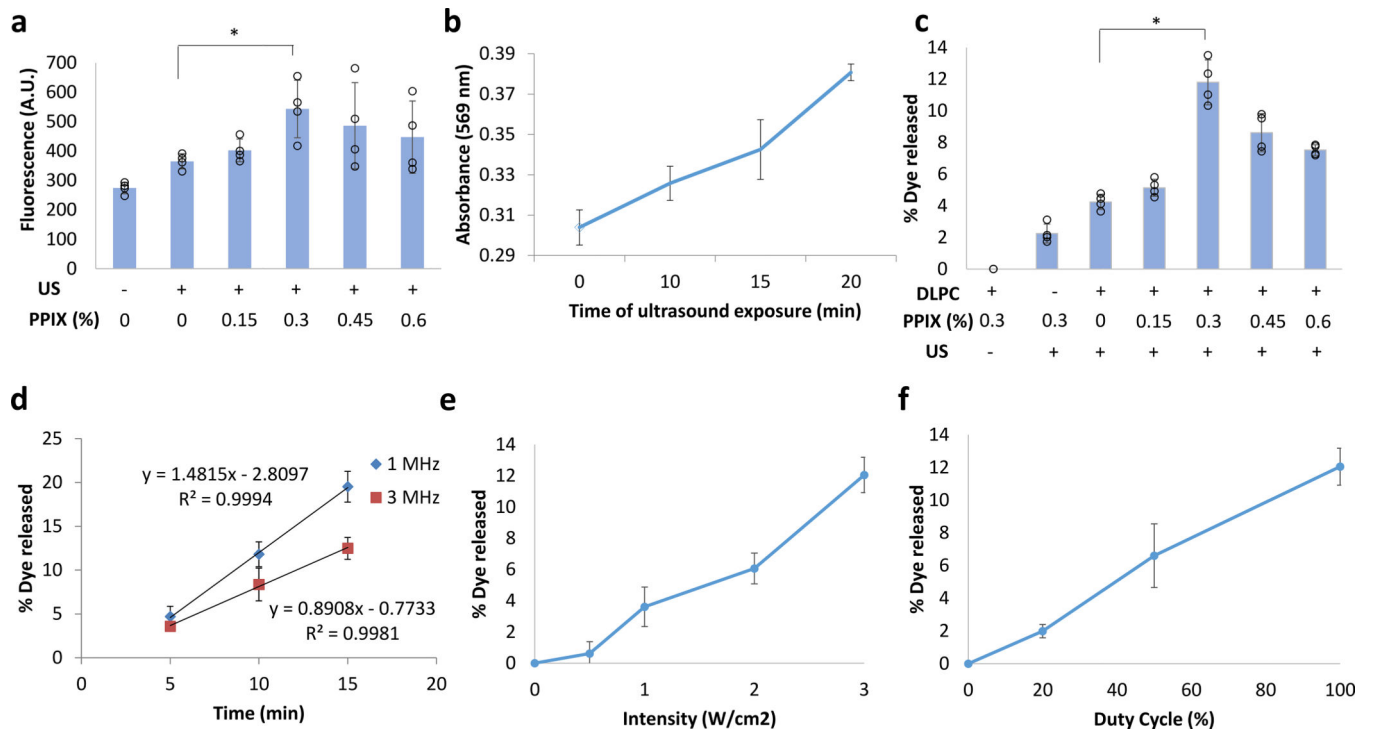
Figure 1.
Ultrasound triggerability with PPIX-loaded liposomes. (a) Effect of PPIX loading on ROS generation (measured by fluorescent assay) by liposomes after 10-min insonation at 1 MHz, 3 W/cm^2. (b) Time course of lipid peroxidation in liposomes of optimal PPIX loading (0.3 % [mg PPIX/mg (PPIX+lipid) × 100 %]) under continuous ultrasound (US) exposure (3 W/cm^2, 1 MHz). See *Methods* for details. (c) Effect of PPIX loading in liposomes (mg PPIX/mg lipid+PPIX × 100 %) and of presence of DLPC on sulforhodamine B release after insonation (3W/cm^2, continuous application, 1 MHz, 10 min). (d–f) *In vitro* dye release as a function of (d) ultrasound duration and frequency (3W/cm^2, continuous application), (e) ultrasound intensity (10 min, 1 MHz, continuous application), and (f) duty cycle (1 MHz, 10 min, 3 W/cm^2). Data are means ± SD, N=4. *P<0.05. All individual data points are listed in Table S6–S11.
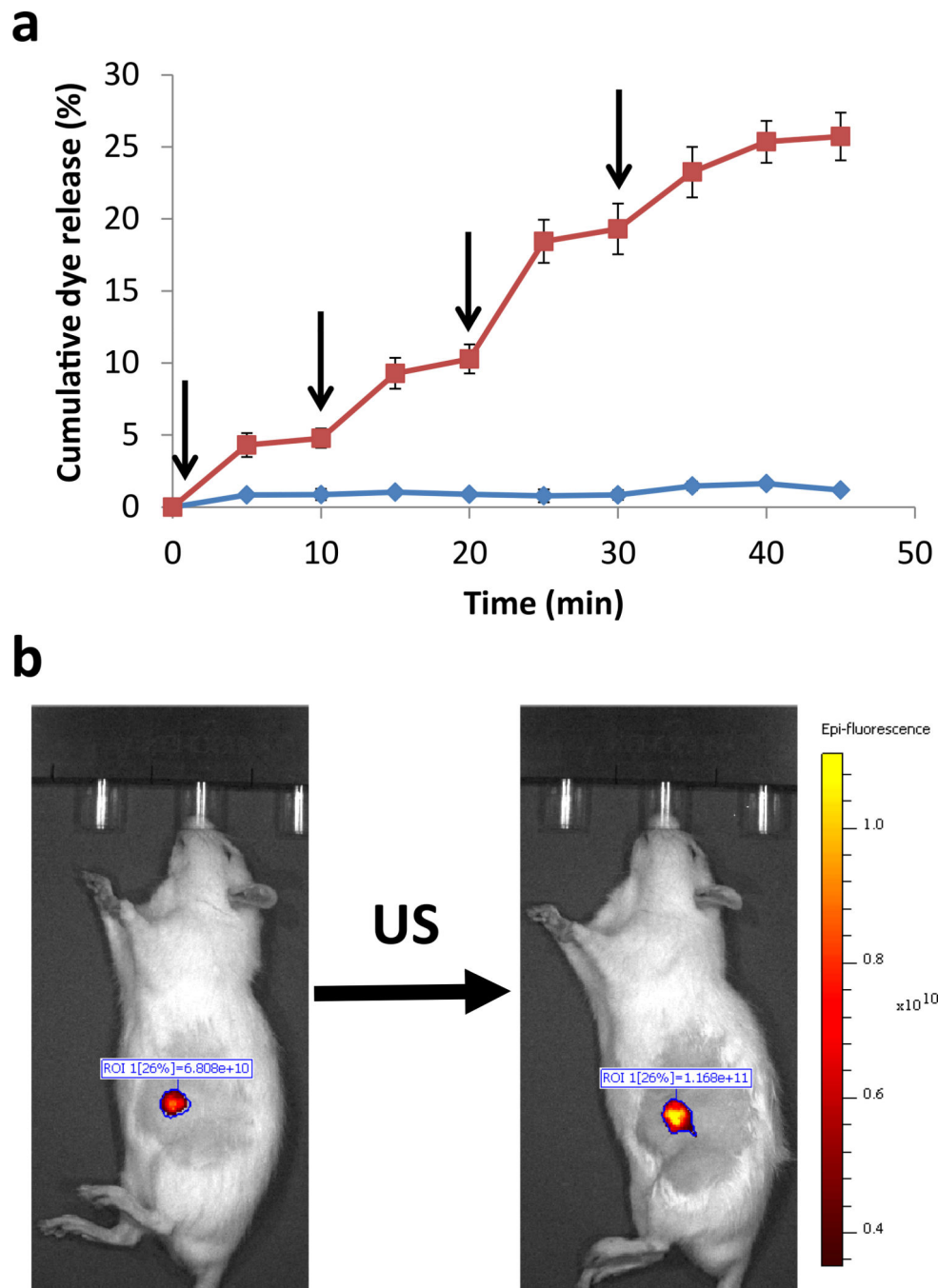
Figure 2.
Ultrasound (US)-triggered dye release from Lipo-PPIX-SRho. (a) Repeated ultrasound-triggered dye release (cumulative % of total); insonation (5 min, 1 MHz, 3W/cm^2, continuous) is indicated by arrows. Data are means ± SD. N=5 for no US group, N=6 for US group. Individual data points are listed in Table S12–S13. (b) Ultrasound triggering of dye release from subcutaneously injected Lipo-PPIX-SRho (1 MHz, 10 min, continuous application, 3 W/cm^2), N=4; P < 0.001 for comparison of the average integrated

epifluorescence of non-ultrasound triggered and ultrasound-triggered animals. Individual data points are listed in Table S14.
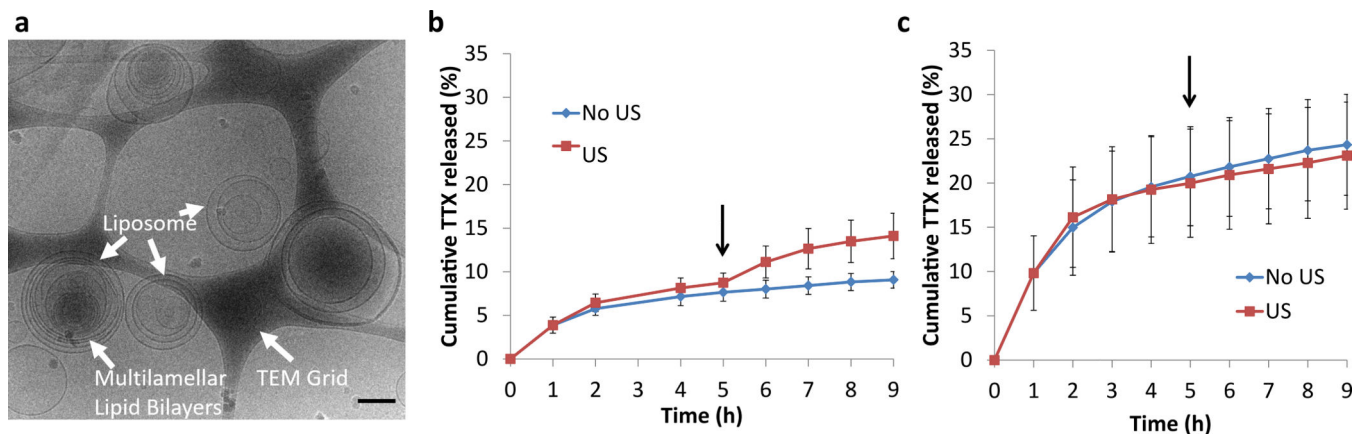
Figure 3.
TTX-loaded liposomes. (a) Representative cryo-transmission electron microscopy micrograph of Lipo-PPIX-TTX. Scale bar = 200 nm. (b–c) *In vitro* TTX release (cumulative % of total) at 37°C from (b) Lipo-PPIX-TTX and (c) Lipo-TTX with and without ultrasound (US). Arrows represent the application of ultrasound (1 MHz, 3 W/cm^2, continuous, 10 min) at the 5 h time point. Data are means ± SD, N = 4. All individual data points are listed in Table S15–S16. At 9 h of incubation, P=0.005 in panel b and P=0.39 in panel c for the comparison between samples with and without insonation.
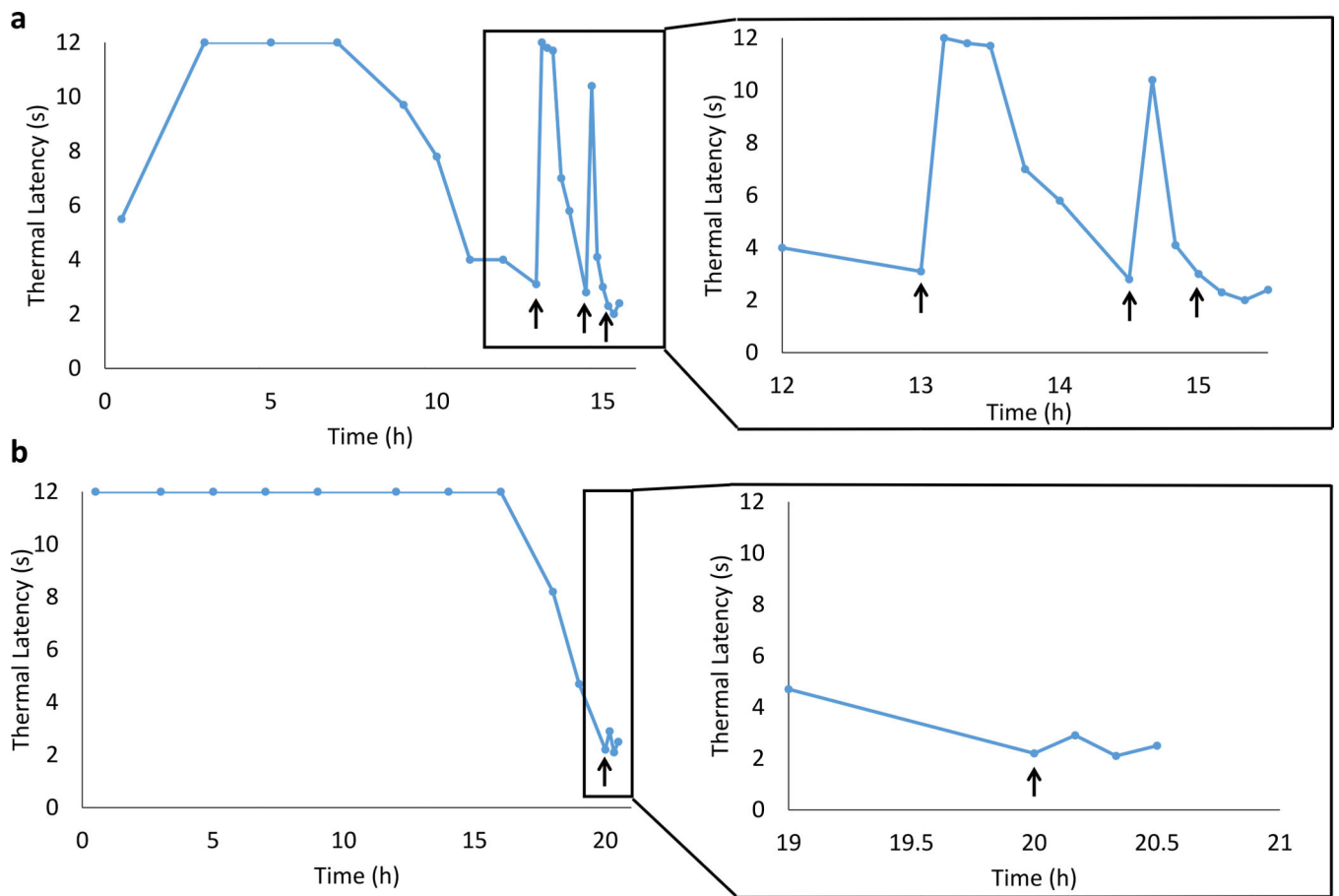
Figure 4.
Representative (from one animal of 4) timecourses of thermal latency after injection of liposomal formulations and subsequent insonation. Animals were injected with 200 μL of (a) Lipo-PPIX-TTX, or (b) Lipo-TTX. Insonation (3 W/cm^2, 1 MHz, 10 min) is indicated by black arrows. The triggered nerve blocks are magnified to the right. Individual data points for all animals are listed in Table S17–S18.
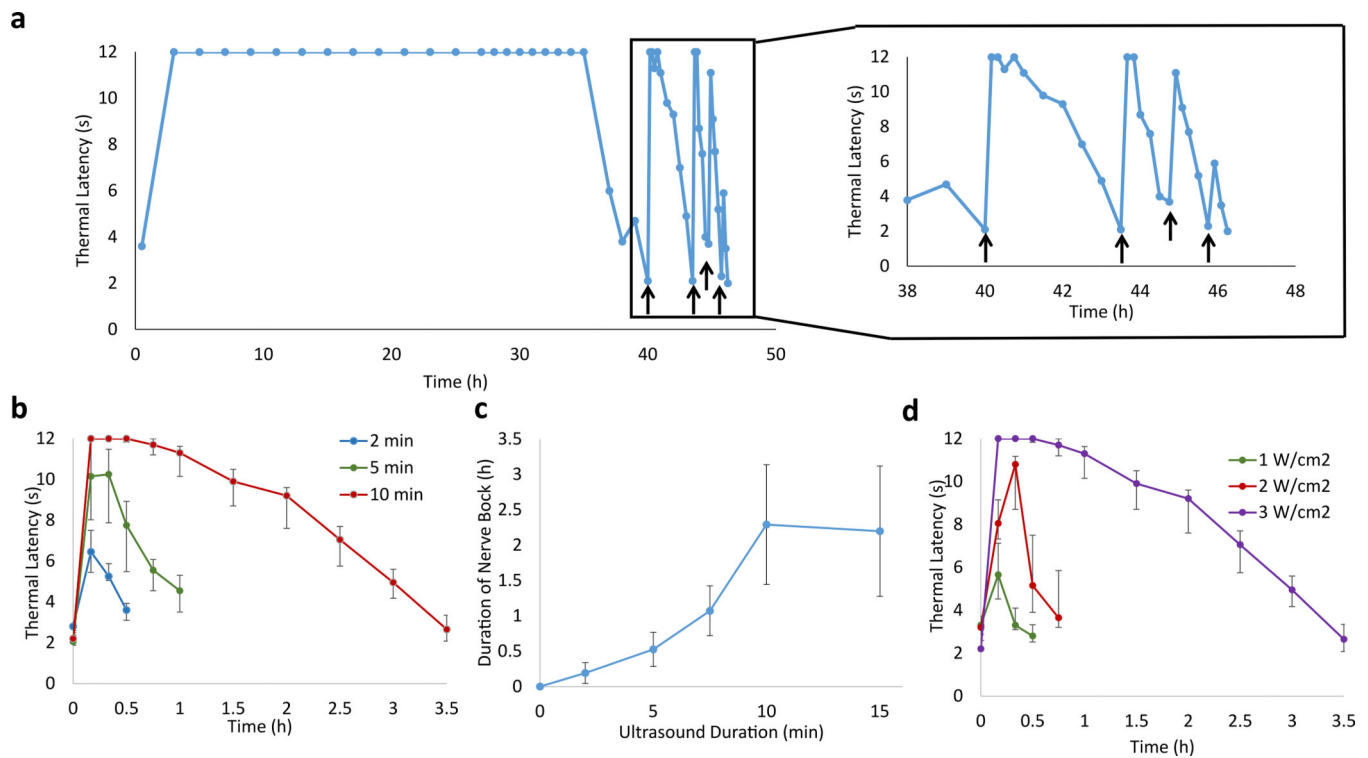
Figure 5.
Effect of ultrasound on thermal latency after injection of Lipo-PPIX-TTX + Lipo-DMED and subsequent insonation. (a) Representative (from 1 of 4 rats) timecourse with 10-min insonations (black arrows, 1 MHz, continuous application, 3 W/cm^2). The triggered nerve blocks are magnified to the right. Individual data points for all 4 animals are listed in Table S18. (b) Effect of insonation duration (2, 5, or 10 min) on the timecourse of the first ultrasound-triggered nerve block (after the initial nerve block wore off). Data are medians ± quartiles, N=4. (c) Effect of duration of insonation on the duration of the first triggered nerve block. Data are means ± SD, N=4. (d) Effect of insonation intensity (10 min and 1, 2, or 3 W/cm^2) on the timecourse of the first ultrasound-triggered nerve block (after the initial nerve block wore off). Data are medians ± quartiles, N=4. Individual data points from all animals are listed in Table S19–S22.
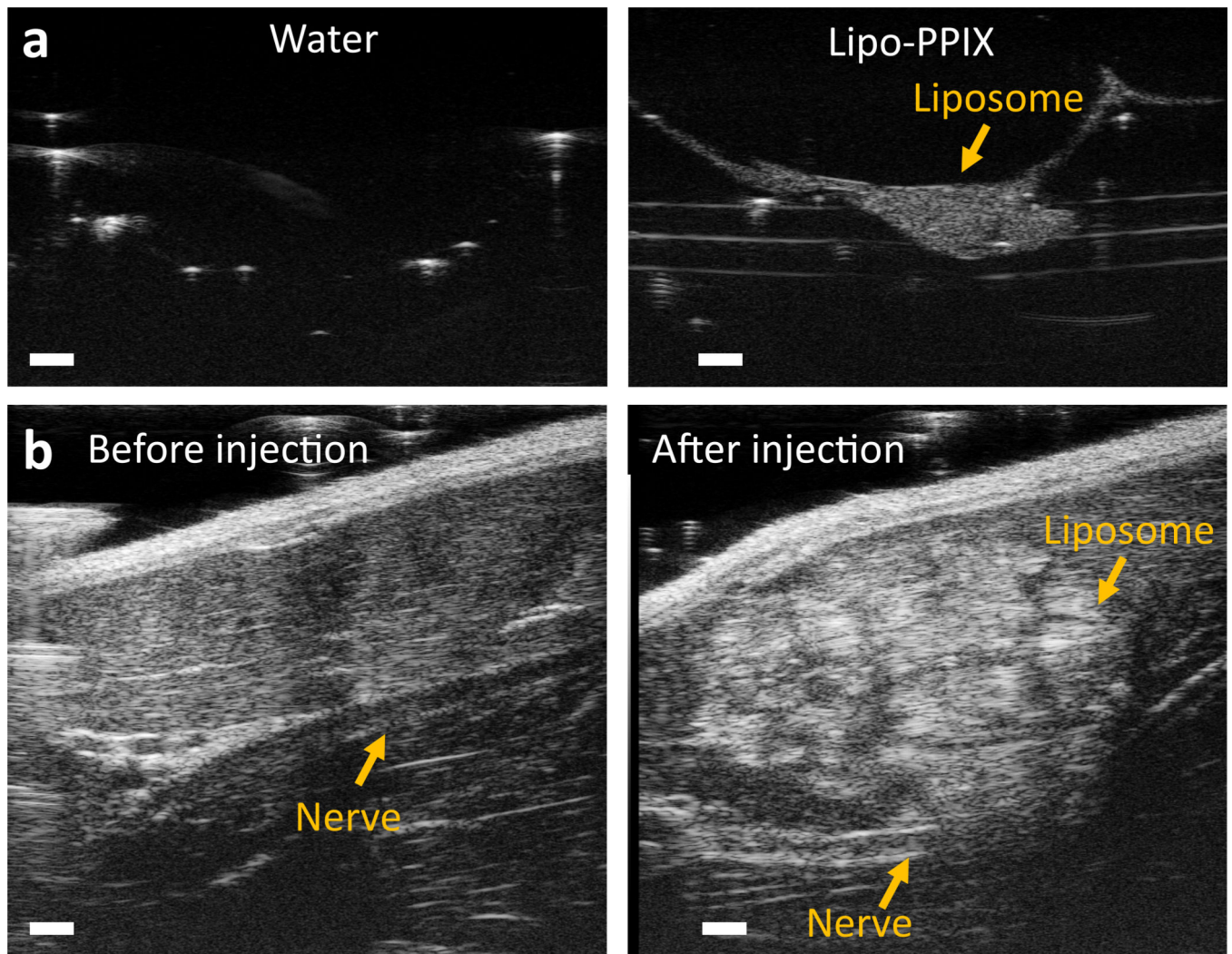
Figure 6.
Ultrasonography of Lipo-PPIX. (a) *In vitro* comparison of echogenic contrast of Lipo-PPIX-TTX and water. (b) Sonograms before and after ultrasound guided perisciatic injections of Lipo-PPIX. Sonograms were taken with a 40-MHz ultrasound transducer. Scale bars are 1 mm.